A High Frequency Signal Injection based Optimum Reference Flux Searching for Direct Torque Control of a Three-Level Traction Drive

Mohammad Hazzaz Mahmud, Yuheng Wu, Waleed Alhosaini, Fei Diao, and Yue Zhao
Power Electronic Systems Laboratory at Arkansas (PESLA)
University of Arkansas
Fayetteville, AR, 72701 USA
mhmahmud@uark.edu, yuhengwu@uark.edu, wsalhosa@uark.edu, feidiao@uark.edu, yuezhao@uark.edu

***Abstract*—Direct torque control (DTC) is widely used in both industries and academia due to its distinctive advantages, e.g., fast dynamic response and high robustness against motor parameters uncertainties and external disturbances. However, there are also some major drawbacks of conventional DTC, such as large torque ripples and poor efficiency caused due to the use of non-optimal flux references. This paper proposes a model-free extremum seeking control (ESC) algorithm for a three-level (3-L) inverter to reduce torque ripples and improve the drive efficiency. Firstly, the relationship between the stator flux linkage and the magnitude of stator current is analyzed. Then, based on this relationship, an effective high frequency signal injection (HFSI) based ESC algorithm is proposed to determine the optimal reference flux in real-time, leading to a maximum torque per ampere (MTPA) like approach for the 3-L DTC. This method can reduce the time-consuming tuning effort and is very robust to the motor parameters variations. The feasibility and effectiveness of proposed methods are verified by using both simulation and experimental studies.**

Keywords—direct torque control; high frequency signal injection; permanent magnet motor; three level traction drive.

I. INTRODUCTION

The direct torque control (DTC), due to its advantages, such as fast dynamic response and robustness to system uncertainties and nonlinearities [1], has been adopted in various industrial applications. However, when applied to traction applications, the DTC may not be able to ensure optimal operation over the entire operating range and may have high torque ripples, which further lead to poor traction performance and low efficiency respectively [2]. The basic DTC approach needs two references, the torque and flux linkage [3], for the controller to achieve the tracking. The torque and flux both have complex numerical relationship with current vector, the magnetic flux linkage, and inductance of the permanent magnet machines [4]. The most common approach to determine the references is integrating a look-up table (LUT) in the model. However, LUT suffers from parameter variations [5]. This technique cannot ensure the optimal operating condition all the time due to magnetic saturation in the motors. To address these issues, a direct calculation method of reference flux linkage to realize MTPA for DTC is presented in [5], which relies on the mathematical machine model in the *d-q* frame and also machine parameters. To eliminate the dependency of machine parameters on MTPA, signal injection based methods are proposed in [6]-[7] to detect MTPA points online. In [7], a random frequency signal is added to the reference flux to avoid the residual torque harmonic at the injected signal frequency. Another method is proposed in [8], where a perturb and observe searching algorithm is proposed to determine the optimal reference flux. In [9], an online reference flux correction method is proposed based on the sequential variation of the actual current to an optimal point by correcting the reference stator flux linkage using a local search algorithm to minimize the current. All these signal injection based approaches for MTPA searching are independent to machine parameters, however, the robustness against the ripples and/or noise in torque and stator current is not comprehensively analyzed.

In this paper, an extremum seeking control (ESC) algorithm is proposed for a three-level (3-L) traction inverter to identify the optimal flux linkage in real-time, such that the system efficiency can be enhanced. The ESC [10] is a model-free adaptive control approach, which is often utilized to deal with the system where the reference to output map is not clear but is known to have an extremum. It is an alternative to the offline tuning techniques that are dependent to predetermined information and/or machine model parameters. In the proposed ESC approach, a small high frequency sinusoidal signal in the flux control loop and the system response can be extracted from the stator current, which can be utilized to identify the optimal flux reference. There are various methods to implement the ESC, however maintaining system stability is difficult. In this paper, the proposed ESC algorithm can ensure the effectiveness of optimal reference flux search while maintaining system stability. Comprehensive simulations and experiments are conducted to validate the effectiveness of the proposed control scheme.

II. 3-L DIRECT TORQUE CONTROL

In this paper, the DTC is developed to control a 3-phase 3-L T-type inverter [11]. Fig. 1 shows all the 18 active voltage vectors that a 3-L inverter could generate, where the output of the inverter could be represented by the combination of "P", "O", and "N", which are corresponding to $+V_{dc}/2$, 0, and $-V_{dc}/2$, respectively. An example is given in Fig. 1 to show the influences of applying different voltage vectors on torque and

This work was supported in part by the U.S. National Science Foundation (NSF) under CAREER Award ECCS-1751506.

flux. Based on the influence, the optimal voltage vector can be selected. Fig. 2 is an illustration of the 3-L DTC approach which also includes the proposed ESC algorithm to generate the optimized flux reference for the flux controller. The 3-L DTC mainly includes hysteresis controllers for the stator flux linkage and the electromagnetic torque and their corresponding estimators, a sector detection block and a switching table. Based on the flux tracking error, output of the stator flux controller which is defined as τ selects active voltage vectors to maintain the flux trajectory within the pre-determined hysteresis band. Similarly, the output of the torque controller which is presented as ʌ in Fig.2 selects both active and null vectors based on torque tracking error to ensure the output torque tracks its reference. The flux and torque control is achieved by using hysteresis and look-up table (LUT) [9], and a PI controller in the torque control loop is designed to eliminate the steady-state error caused by the dead zone (which is 10 ~ 15% of the rated torque) in the LUT [12]. Table I has the switching LUT for the 3-L DTC. Proper voltage vector is selected according to the LUT based on sectors, flux and torque reference.

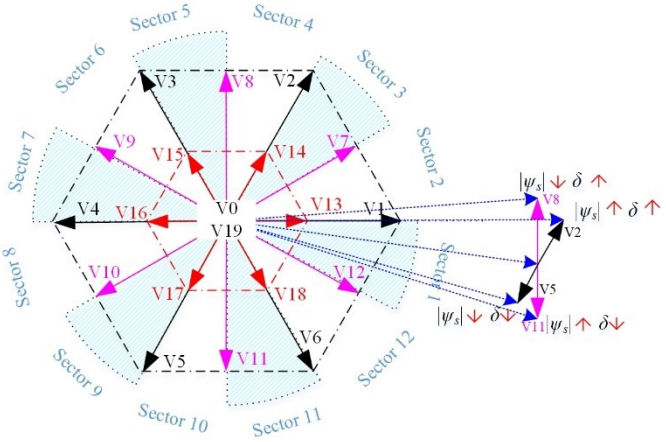

Fig. 1. The selection of voltage vector.

TABLE I. SWITCHING TABLE

	ʌ	+1				-1			
	τ	+2	+1	-1	-2	+2	+1	-1	-2
Sector	1	V_2	V_{14}	V_{18}	V_8	V_{11}	V_{15}	V_{17}	V_5
	2	V_8	V_{14}	V_{18}	V_6	V_3	V_{15}	V_{17}	V_{11}
	3	V_3	V_{15}	V_{13}	V_9	V_{12}	V_{16}	V_{18}	V_6
	4	V_9	V_{15}	V_{13}	V_1	V_4	V_{16}	V_{18}	V_{12}
	5	V_4	V_{16}	V_{14}	V_{10}	V_7	V_{17}	V_{13}	V_1
	6	V_{10}	V_{16}	V_{14}	V_2	V_5	V_{17}	V_{13}	V_7
	7	V_5	V_{17}	V_{15}	V_{11}	V_8	V_{18}	V_{14}	V_2
	8	V_{11}	V_{17}	V_{15}	V_3	V_6	V_{18}	V_{14}	V_8
	9	V_6	V_{18}	V_{16}	V_{12}	V_9	V_{13}	V_{15}	V_3
	10	V_{12}	V_{18}	V_{16}	V_4	V_1	V_{13}	V_{15}	V_9
	11	V_1	V_{13}	V_{17}	V_7	V_{10}	V_{14}	V_{16}	V_4
	12	V_7	V_{13}	V_{17}	V_5	V_2	V_{14}	V_{16}	V_{10}

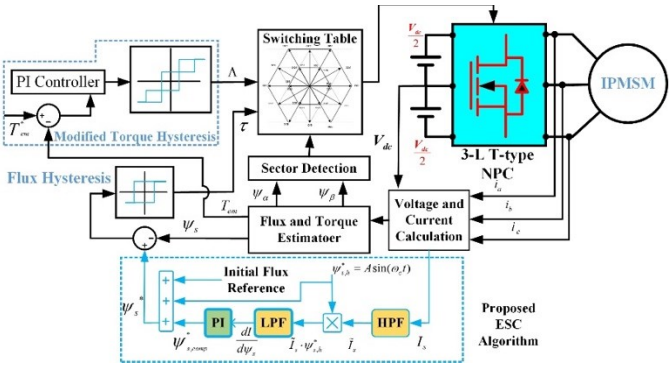

Fig. 2. A block diagram of 3-L DTC with ESC algorithm.

III. THE PROPOSED ESC ALGORITHM FOR OPTIMAL FLUX SEARCHING

A. *Relationship Between Optimal ψ_s* and MTPA Points*

Considering a generic interior permanent magnet (IPM) motor, the stator current, $|I_s|$, and flux linkage, $|\psi_s|$, can be written as a function of the *d*-axis current id, i.e., $f(i_d)$ and $g(i_d)$, respectively [7]

$$|I_s| = \sqrt{i_d^2 + \frac{4}{9}\frac{T_{em,0}^2}{P^2[\psi_m + (L_d - L_q)i_d]^2}} = f(i_d) \quad (1)$$

$$|\psi_s| = \sqrt{(\psi_m + L_d i_d)^2 + \frac{4}{9}\frac{L_q^2 T_{em,0}^2}{P^2[\psi_m + (L_d - L_q)i_d]^2}} = g(i_d) \quad (2)$$

where L_d and L_q are *d*- and *q*- axis inductances, respectively; ψ_m is the flux linkage produced by the permanent magnets; T_{em} is the electromagnetic torque; P is the number of pole-pairs and i_q is the *q*- axis current. The relationship between i_d and i_q for MTPA trajectory can be expressed as

$$i_d = \frac{\psi_m}{2(L_q - L_d)} - \sqrt{\frac{\psi_m^2}{4(L_q - L_d)^2} + i_q^2} \quad (3)$$

A numerical simulation was performed to reveal the relationship between $|I_s|$ and $|\psi_s|$, which is shown in Fig. 3. The IPM machine parameters used in simulation are summarized in Tables II. As shown in Fig. 3, the red circle means the optimum flux at a given torque reference that requires minimum stator current. Thus, the aim of the ESC scheme is to find the optimum flux in real-time.

TABLE II. MACHINE PARAMETERS

Nominal Power	150 kW
Maximum torque	300 Nm
Flux linkage	0.095 Wb
Average L_d	0.2 mH
Average L_q	0.55 mH
Base speed	5000 RPM
Pole-pair number	4
Stator resistance	0.01 Ω

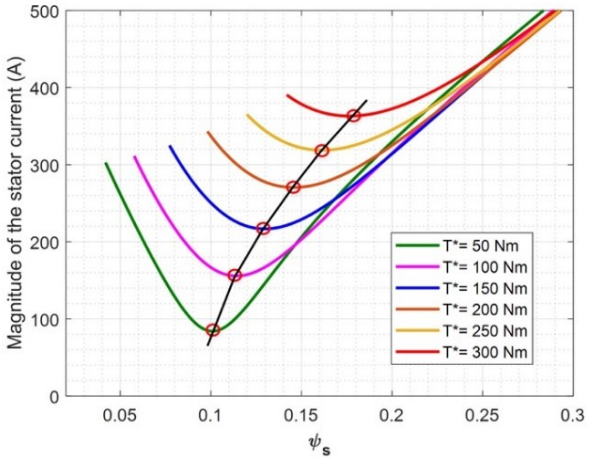

Fig. 3. The profiles of $|I_s|$ Vs. $|\psi_s|$ at different torque operating points.

B. *Extremum Seeking Control Algorithm for Optimal ψ_s^* Searching*

In this work, an ESC algorithm is proposed to find the optimal ψ_s^* online, as shown in Fig. 2. This flux searching approach does not require prior knowledge of drive system. During the search process, a pulsating signal, $A\sin(\omega_c t)$, where A is the amplitude and ω_c is pulsating frequency, is injected and superposed onto the original stator flux reference $\psi_{s,0}^*$. Fig. 4 shows the operating principle of the proposed ESC scheme. According to Fig. 4, when $\psi_{s,h}^*$ is injected, high frequency response can be found in the stator current, which can be expressed as

$$I_s \approx \bar{I}_s + \tilde{I}_s \approx \bar{I}_s + \frac{dI_s}{d\psi_s}\cdot \sin(\omega_c t) \tag{4}$$

where $\bar{I}_s$ stands for the steady state response to $\psi_{s,0}^*$ and is the high frequency response due to $\psi_{s,h}^*$. As shown in Fig. 4, the stator current may have different responses to the injected high $\psi_{s,h}^*$, which depends on the operating point. When IPM operates at the left hand side of the MTPA operating point, $dI_s/d\psi_s$ is negative, vice versa. If IPM operates exactly at MTPA operating point, theoretically $dI_s/d\psi_s$ is 0. The block diagram of the proposed ESC is shown in Fig. 2. The magnitude of stator current can be extracted from the measured phase currents i_a, i_b and i_c. As Fig. 2 shows, in the ESC scheme, the stator currents I_s will go through a high-pass filter to obtain the high frequency components of I_s, which contains the information of $dI_s/d\psi_s$. In this work, the cutoff frequency of the HPF is 1 kHz. However, in $\tilde{I}_s$, $dI_s/d\psi_s$ is modulated by the injected high frequency sinusoidal signal, whose frequency is 2 kHz. To extract the information of $dI_s/d\psi_s$, a demodulator is designed using $\psi_{s,h}^*$ as

$$\tilde{I}_s \cdot \psi_{s,h}^* = A^2 \cdot \frac{dI_s}{d\psi_s}\cdot \sin^2(\omega_c t) = \frac{A^2}{2}\frac{dI_s}{d\psi_s} - \frac{A^2}{2}\frac{dI_s}{d\psi_s}\sin(2\omega_c t) \tag{5}$$

As shown in (5), the output of the demodulator contains a dc term, which is proportional to $dI_s/d\psi_s$, and a high frequency term. Then a low-pass filter is utilized to extract the dc term. To ensure the optimal operating, in this work, a proportional-integral (PI) controller is designed to enforce $dI_s/d\psi_s$ to be zero.

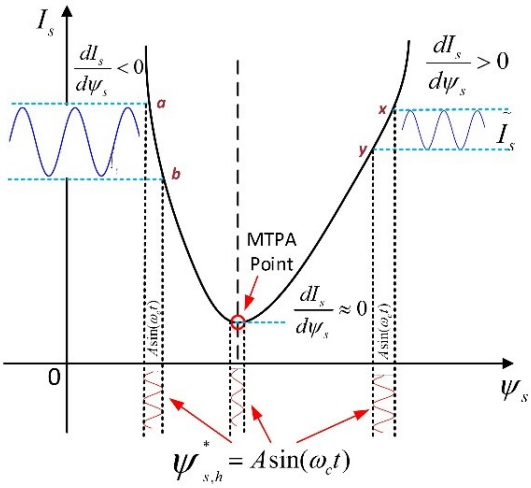

Fig. 4. An illustration for the response of the stator current to injected high frequency stator flux.

$$\psi_{s,comp}^* = \left(k_p + \frac{k_i}{s}\right)\cdot \frac{dI_s}{d\psi_s} \tag{6}$$

where k_p and k_i are the PI gains. The output of PI stage, i.e., $\psi_{s,comp}^*$, is used as a compensation term in the stator flux reference, i.e.,

$$\psi_s^* = \psi_{s,0}^* + \psi_{s,comp}^* + \psi_{s,h}^* \tag{7}$$

IV. Simulation and Experimental Results

A. *Simulation Studies*

In this section, simulation results are presented to validate the 3-L DTC with proposed ESC algorithm for optimal reference flux identification. The machine parameters used in the simulation are identical to those presented in Table II. The motor mechanical speed was kept constant at 157 rad/sec with a varying torque reference. The theoretical optimal stator flux is around 0.12 V·s when T^* = 150 Nm. The frequency of the injected signal, ω_c is set as 2 kHz, and the amplitude is A = 0.001425 in this work. The sampling frequency of the DTC algorithm in the simulation studies is 65 kHz.

Fig. 5 shows the simulation results where the ESC algorithm is activated at t = 0.1s. It shows the reference vs. estimated torque throughout the whole simulation. When the ESC is activated, the torque remains constant firstly. Then a step change in load torque is applied from 150 Nm to 250 Nm at 0.2 s. Fig. 6 shows the three-phase stator current, which reduced to 280 A from 220 A while the ESC is activated at 0.1 s. From Fig. 7, it is obvious that the reference flux, ψ_s^* changes from its initial value to the optimal point for both torque command.

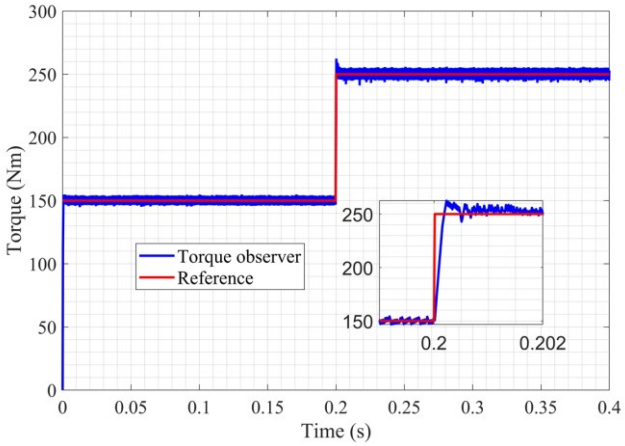

Fig. 5. Reference vs. estimated torque.

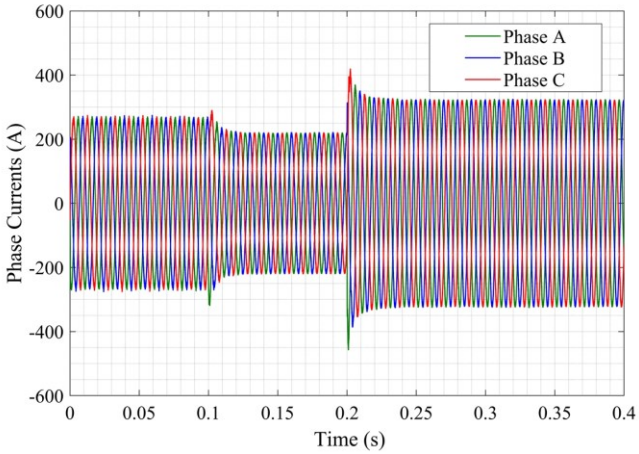

Fig. 6. Three phase stator currents.

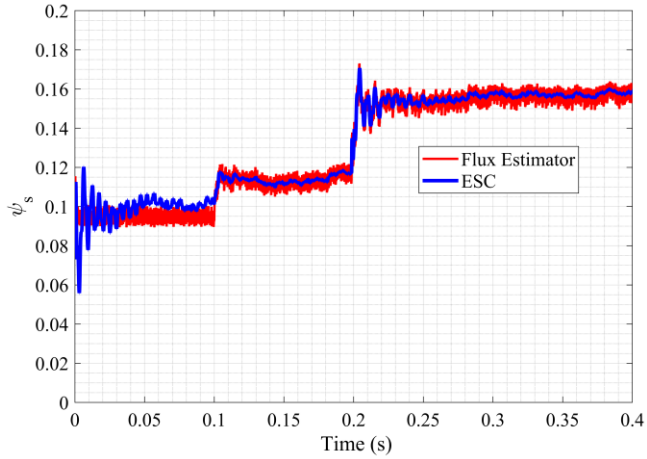

Fig. 7. Estimated flux vs. flux reference generated by ESC algorithm.

Fig. 8 shows the α, β flux trajectory. Fig. 9 indicates the current THD (%) vs. the amplitude of the injected signal, $\Delta\psi_s$ which is identical to the A discussed earlier, and Fig. 10 shows the relationship between the settling time of ESC vs. $\Delta\psi_s$. It is clear that THD (%) increases linearly with $\Delta\psi_s$, when $\Delta\psi_s$ is greater than 1% of the reference stator flux, whereas, settling time of the ESC is inversely related to $\Delta\psi_s$. Therefore, it is possible to select an appropriate $\Delta\psi_s$ based on the information given in Fig. 9 and 10. For instance, if $\Delta\psi_s$ = 0.00285 is selected, settling time is only 0.02 s but the current THD would be 4.2%. On the other hand, if $\Delta\psi_s$ = 0.00475 is selected, settling time would be 0.3 s that is much longer than the previous case, however the current THD is only 2.2%. It is a tradeoff between the current THD and settling time. In this paper $\Delta\psi_s$ = 0.001425 is selected as the amplitude of the injected signal.

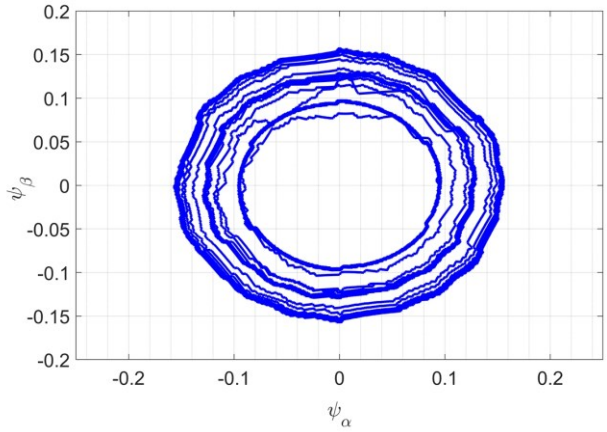

Fig. 8. α, β flux trajectory.

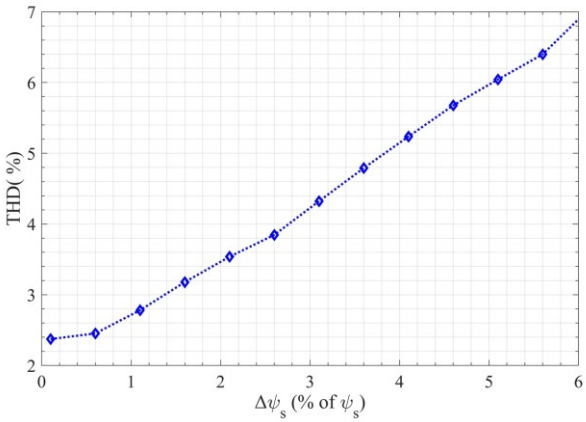

Fig. 9. THD (%) vs. $\Delta\psi_s$.

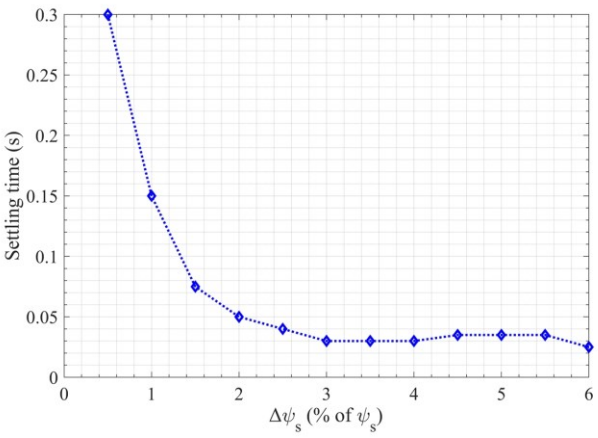

Fig. 10. Settling time of the ESC algorithm vs. $\Delta\psi_s$.

B. *Experimental Studies*

To further validate the effectiveness of the proposed ESC algorithm and the resulting 3-L DTC drive, experimental studies are performed. The experiment was carried out on a scaled down prototype of all-SiC T-type inverter. A 300 W IPM motor was used in the experiment with major parameters as, $R = 0.27\ \Omega$, $L_d = 1.12$ mH, $L_q = 1.58$ mH, $\psi_m = 0.034$ V·s, and number of the pole-pairs is 2. The overall ESC control algorithm and DTC are implemented in ds1103 dSPACE real time control system.

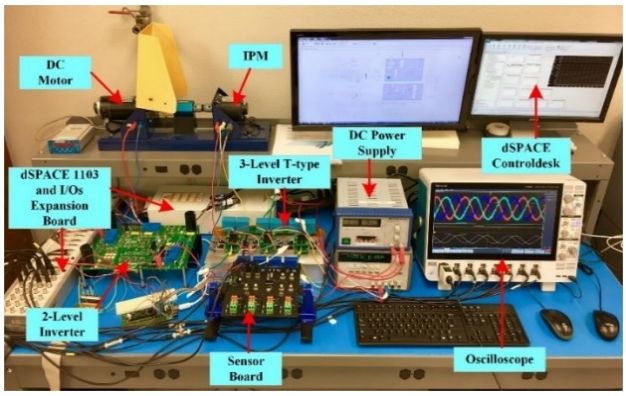

Fig. 11. Experimental setup.

The overall experimental setup is shown in Fig. 11. The setup consists of an IPM motor controlled by a three-level T-type inverter, and a DC motor is also adopted to drive the IPM motor and keep a constant speed, which is controlled by a two-level H-bridge converter. Besides the proposed ESC based 3-level DTC scheme, the DC motor controller is also realized in the dSPACE platform. The sampling frequency of the DTC is 65 kHz at motor shaft speed of 50 rad/sec. Fig. 12 shows the comparison between the simulation and experimental results to demonstrate the relationship between the magnitude of the stator current and the magnitude of the stator flux linkage ψ_s when the torque reference is 0.4 Nm. In Fig. 12, the blue line indicates the profile obtained from simulation, and red line indicates the data extracted from the experiment. When accurate machine parameters are used, both simulations data and experimental test points are very close to each other.

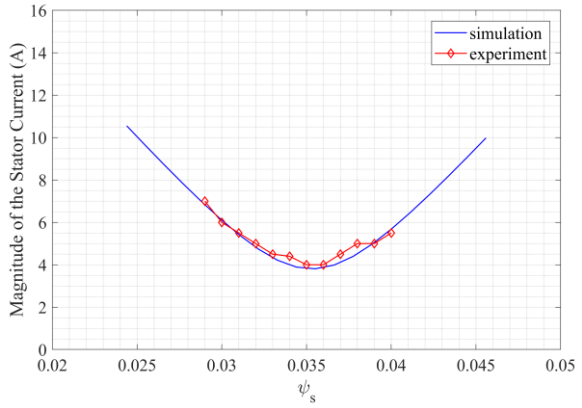

Fig. 12. Simulation (blue line) vs. experimental (red line) result comparison at $T^* = 0.4$ Nm.

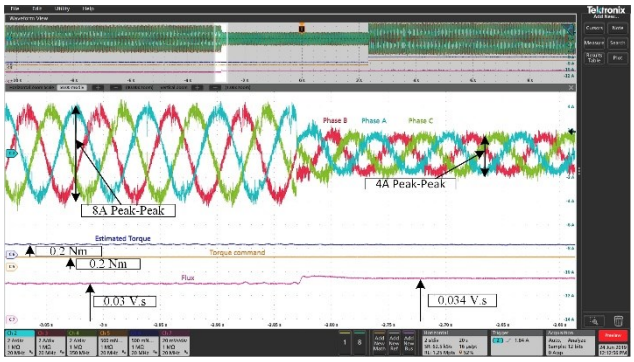

Fig. 13. Experimental results of three-phase stator currents, torque and $|\psi_s|$ at $T^* = 0.2$ Nm.

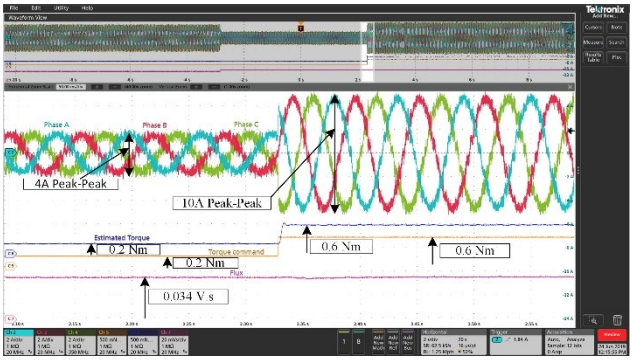

Fig. 14. Dynamic response of the system $|\psi_s|$ while the ESC algorithm is activated by step changing of torque from 0.2 Nm to 0.6 Nm.

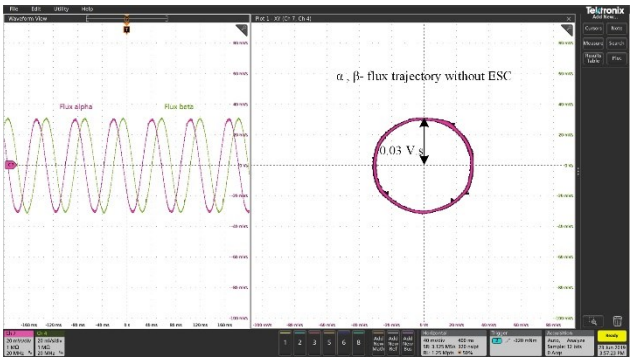

Fig. 15. α-, β-flux trajectory without ESC.

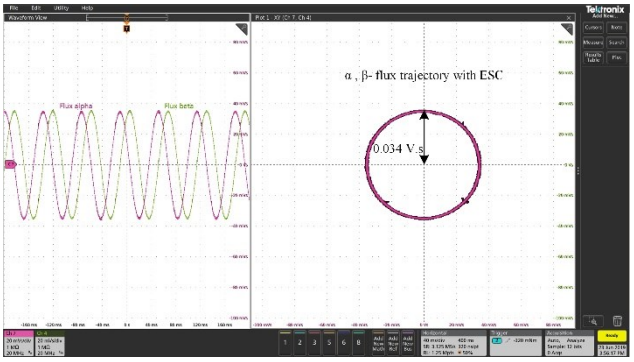

Fig. 16. α-, β-flux trajectory with ESC.

Fig. 13 shows the experimental results of three-phase stator currents, torque and magnetic flux. Initially the flux reference was set to be 0.03 V.s, while the ESC algorithm is deactivated; the IPM motor operates in a non-optimal operating condition, which is indicated by the magnitude of the stator currents shown in Fig. 13. Once the ESC algorithm is enabled, the flux linkage reaches to its optimum within 6 ms, and the output torque remained constant. Because of the ESC algorithm, the RMS value of the stator current is reduced to 1.4 A from 2.8 A. Fig. 14 shows the dynamic response of the system while ESC is always active. In this case, a step change in the torque reference from 0.2 Nm to 0.6 Nm is applied. The torque of the IPM motors well tracks its reference with optimal stator currents. The results presented in Fig. 15 and Fig. 16, show the α-, β-flux linkage trajectories before and after activating the proposed ESC respectively. Both simulation and experimental results validate the effectiveness of the ESC algorithm for DTC of IPM machine.

V. Conclusion

In this paper, the relationship between the magnitude of the stator flux linkage and the magnitude of the stator current has been developed by numerical analysis. Then an effective ESC algorithm is proposed to determine the optimal reference flux linkage online, leading to a MTPA-like approach for DTC of IPM motors. The proposed method can significantly reduce the time consuming tuning effort and is robust to motor parameters variations. Also, the proposed control technique can result in improvement in the system efficiency. The simulation and experimental results are presented to validate the feasibility and effectiveness of proposed method.

References

[1] G. S. Buja, and M. P. Kazmierkowski, “Direct Torque Control of PWM Inverter-Fed AC Motors - A Survey,” IEEE Transactions on Industrial Electronics, Vol. 51,No. 4, pp. 744-757, Aug. 2004.

[2] G. Abad, M. A. Rodriguez, and J. Poza, “Two-Level VSC Based Predictive Direct Torque Control of the Doubly Fed Induction Machine With Reduced Torque and Flux Ripples at Low Constant Switching Frequency,” IEEE Transactions on Power Electronics, Vol. 23, No. 3, pp. 1050–1061, May 2008.

[3] M. R., Barzegaran, M., Kamruzzaman, H., Mahmud, and O. A., Mahmud, "Direct torque control of permanent magnet synchronous machine using Sparse matrix converter with SiC switches." 2015 IEEE International Electric Machines & Drives Conference (IEMDC). IEEE, 2015.

[4] A. Shinohara, Y. Inoue, S. Morimoto and M. Sanada, "Maximum Torque Per Ampere Control in Stator Flux Linkage Synchronous Frame for DTC-Based PMSM Drives Without Using q-Axis Inductance," IEEE Transactions on Industry Applications, Vol. 53, No. 4, pp. 3663-3671, July-Aug. 2017.

[5] A. Shinohara, Y. Inoue, S. Morimoto and M. Sanada, "Direct Calculation Method of Reference Flux Linkage for Maximum Torque per Ampere Control in DTC-Based IPMSM Drives," IEEE Transactions on Power Electronics, Vol. 32, No. 3, pp. 2114-2122, March 2017.

[6] A. Shinohara, Y. Inoue, S. Morimoto and M. Sanada, “Correction of reference flux for MTPA control in direct torque controlled interior permanent magnet synchronous motor drives,” Proc. IEEE IPEC, pp. 324–329, 2014.

[7] S. Bolognani, L. Peretti, and M. Zigliotto, “Online MTPA control strategy for DTC synchronous-reluctance-motor drives,” IEEE Transactions on Power Electronics., Vol. 26, No. 1, pp. 20‑28, Jan. 2011.

[8] Y. Zhao, M. H. Mahmud, and L. Wang, “An Online Optimal Reference Flux Searching Approach for Direct Torque Control of Interior Permanent Magnet Synchronous Machines,” Proc. IECON 2017-43rd Annual Conference of the IEEE Industrial Electronics Society, 2017, pp. 1790-1795.

[9] D. Mohan, X. Zhang, and G. H. B. Foo, “Three-Level Inverter-Fed Direct Torque Control of IPMSM With Constant Switching Frequency and Torque Ripple Reduction,” IEEE Transactions on Industrial Electronics, Vol. 63, No. 12, pp. 7908-7918, Dec. 2016.

[10] M. Hamza, “Extremum Control of Continuous Systems,” IEEE Transactions on Automatic Control, Vol. 11, No. 2, pp. 182-189, Apr. 1966.

[11] Z. Wang, M. H. Mahmud, M. H. Uddin, B. McPherson, B. Sparkman, Y. Zhao, and J. R. Fraley, “A Compact 250 kW Silicon Carbide MOSFET based Three-Level Traction Inverter for Heavy Equipment Applications,” Proc. 2018 IEEE Transportation Electrification Conference and Expo (ITEC), 2018, pp. 1129-1134.

[12] Z. Q. Zhu, Y. Ren, and J. Liu, “Improved torque regulator to reduce steady-state error of torque response for direct torque control of permanent magnet synchronous machine drives,” IET Electric Power Applications, Vol. 8, No. 3, pp. 108-116, Mar. 2014.